

13

Switched Reluctance Machines

Iqbal Husain
The University of Akron

- 13.1 [Introduction](#)
Advantages • Disadvantages
- 13.2 [SRM Configuration](#)
- 13.3 [Basic Principle of Operation](#)
Voltage Balance Equation • Energy Conversion • Torque
Production • Torque–Speed Characteristics
- 13.4 [Design](#)
- 13.5 [Converter Topologies](#)
- 13.6 [Control Strategies](#)
Control Parameters • Advance Angle Calculation •
Voltage-Controlled Drive • Current-Controlled
Drive • Advanced Control Strategies
- 13.7 [Sensorless Control](#)
- 13.8 [Applications](#)

13.1 Introduction

The concept of switched reluctance machines (SRMs) was established as early in 1838 by Davidson and was used to propel a locomotive on the Glasgow–Edinburgh railway near Falkirk [1]. However, the full potential of the motor could not be utilized with the mechanical switches available in those days. The advent of fast-acting power semiconductor switches revived the interest in SRMs in the 1970s when Professor Lawrenson’s group established the fundamental design and operating principles of the machine [2]. The rejuvenated interest of researchers supplemented by the developments of computer-aided electromagnetic design prompted a tremendous growth in the technology over the next three decades. SRM technology is now slowly penetrating into the industry with the promise of providing an efficient drive system at a lower cost.

Advantages

The SRM possess a few unique features that makes it a vigorous competitor to existing AC and DC motors in various adjustable-speed drive and servo applications. The advantages of an SRM can be summarized as follows:

- Machine construction is simple and low-cost because of the absence of rotor winding and permanent magnets.
- There are no shoot-through faults between the DC buses in the SRM drive converter because each rotor winding is connected in series with converter switching elements.

- Bidirectional currents are not necessary, which facilitates the reduction of the number of power switches in certain applications.
- The bulk of the losses appear in the stator, which is relatively easier to cool.
- The torque–speed characteristics of the motor can be tailored to the application requirement more easily during the design stage than in the case of induction and PM machines.
- The starting torque can be very high without the problem of excessive in-rush current due to its higher self-inductance.
- The open-circuit voltage and short-circuit current at faults are zero or very small.
- The maximum permissible rotor temperature is higher, since there are no permanent magnets.
- There is a low rotor inertia and a high torque/inertia ratio.
- Extremely high speeds with a wide constant power region are possible.
- There are independent stator phases, which does not prevent drive operation in the case of loss of one or more phases.

Disadvantages

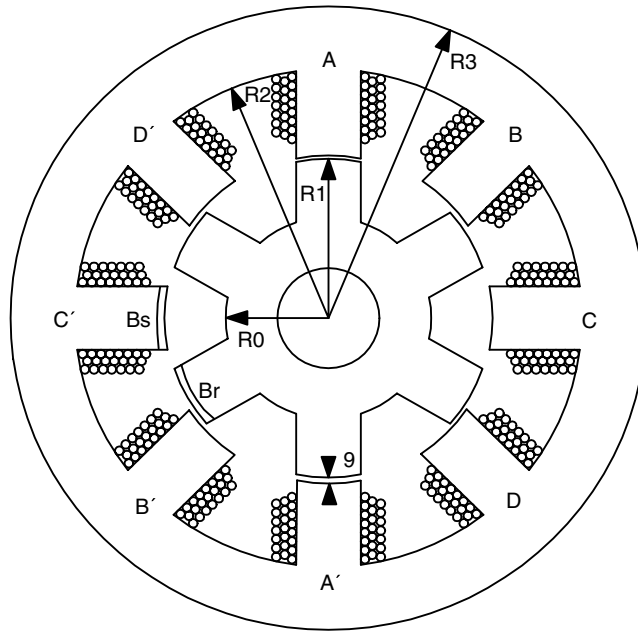
The SRM also comes with a few disadvantages among which torque ripple and acoustic noise are the most critical. The double saliency construction and the discrete nature of torque production by the independent phases lead to higher torque ripple compared with other machines. The higher torque ripple also causes the ripple current in the DC supply to be quite large, necessitating a large filter capacitor. The doubly salient structure of the SRM also causes higher acoustic noise compared with other machines. The main source of acoustic noise is the radial magnetic force induced resonant vibration with the circumferential mode shapes of the stator.

The absence of permanent magnets imposes the burden of excitation on the stator windings and converter, which increases the converter kVA requirement. Compared with PM brushless machines, the per-unit stator copper losses will be higher, reducing the efficiency and torque per ampere. However, the maximum speed at constant power is not limited by the fixed magnet flux as in the PM machine, and, hence, an extended constant power region of operation is possible in SRMs. The control can be simpler than the field-oriented control of induction machines, although for torque ripple minimization significant computations may be required for an SRM drive.

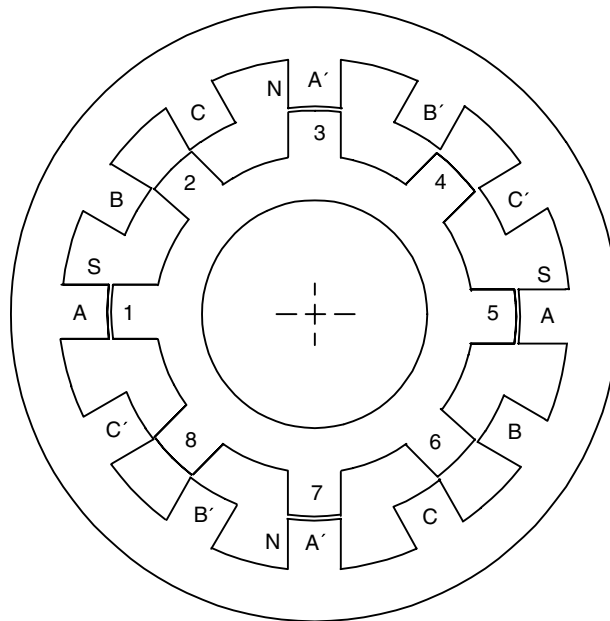
13.2 SRM Configuration

The SRM is a doubly-salient, singly-excited reluctance machine with independent phase windings on the stator, usually made of magnetic steel laminations. The rotor is a simple stack of laminations, without any windings or magnets. The cross-sectional diagrams of a four-phase, 8-6 SRM and a three-phase, 12-8 SRM are shown in Fig. 13.1. The three-phase, 12-8 machine is a two-repetition version of the basic 6-4 structure within the single stator geometry. The two-repetition machine can alternately be labeled as a 4-poles/phase machine, compared with the 6-4 structure with two poles/phase. The stator windings on diametrically opposite poles are connected either in series or in parallel to form one phase of the motor. When a stator phase is energized, the most adjacent rotor pole-pair is attracted toward the energized stator to minimize the reluctance of the magnetic path. Therefore, it is possible to develop constant torque in either direction of rotation by energizing consecutive phases in succession.

The aligned position of a phase is defined to be the situation when the stator and rotor poles of the phase are perfectly aligned with each other attaining the minimum reluctance position. The unsaturated phase inductance is maximum (L_a) in this position. The phase inductance decreases gradually as the rotor poles move away from the aligned position in either direction. When the rotor poles are symmetrically misaligned with the stator poles of a phase, the position is said to be the unaligned position. The phase has the minimum inductance (L_u) in this position. Although the concept of inductance is not valid for a highly saturating machine like SRM, the unsaturated aligned and unaligned inductances are two key reference positions for the controller.



(a)



(b)

FIGURE 13.1 Cross sections of two SR machines: (a) four-phase, 8-6 structure; (b) three-phase, 12-8, two-repetition structure.

Several other combinations of the number of stator and rotor poles exist, such as 10-4, 12-8, etc. A 4-2 or a 2-2 configuration is also possible, but they have the disadvantage that, if the stator and rotor poles are aligned exactly, then it would be impossible to develop a starting torque. The configurations with higher number of stator/rotor pole combinations have less torque ripple and do not have the problem of starting torque.

13.3 Basic Principle of Operation

Voltage Balance Equation

The general equation governing the flow of stator current in one phase of an SRM can be written as

$$V_{\text{ph}} = iR + \frac{d\lambda}{dt} \quad (13.1)$$

where V_{ph} is the DC bus voltage, i is the instantaneous phase current, R is the winding resistance, and λ is the flux linking the coil. The SRM is always driven into saturation to maximize the utilization of the magnetic circuit, and, hence, the flux-linkage λ is a nonlinear function of stator current and rotor position

$$\lambda = \lambda(i, \theta) \quad (13.2)$$

The electromagnetic profile of an SRM is defined by the λ - i - θ characteristics shown in Fig. 13.2. The stator phase voltage can be expressed as

$$V_{\text{ph}} = iR + \frac{\partial \lambda}{\partial i} \frac{di}{dt} + \frac{\partial \lambda}{\partial \theta} \frac{d\theta}{dt} = iR + L_{\text{inc}} \frac{di}{dt} + k_v \omega \quad (13.3)$$

where L_{inc} is the incremental inductance, k_v is the current-dependent back-emf coefficient, and $\omega = d\theta/dt$ is the rotor angular speed. Assuming magnetic linearity (where $\lambda = L(\theta)i$), the voltage expression can be simplified as

$$V_{\text{ph}} = iR + L(\theta) \frac{di}{dt} + i \frac{dL(\theta)}{dt} \omega \quad (13.4)$$

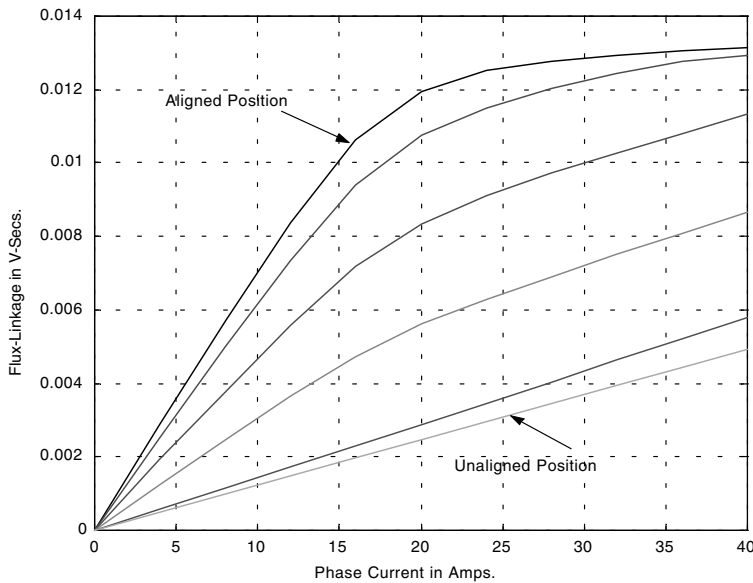


FIGURE 13.2 Flux-angle-current characteristics of a four-phase SRM.

The last term in Eq. (13.4) is the “back-emf” or “motional-emf” and has the same effect on SRM as the back-emf has on DC motors or electronically commutated motors. However, the back-emf in SRM is generated in a different way from the DC machines or ECMs where it is caused by a rotating magnetic field. In an SRM, there is no rotor field and back-emf depends on the instantaneous rate of change of phase flux linkage.

In the linear case, which is always valid for lower levels of phase current, the per phase equivalent circuit of an SRM consists of a resistance, an inductance, and a back-emf component. The back-emf vanishes when there is no phase current or when the phase inductance is constant relative to the rotor position. Depending on the magnitude of current and rotor angular position, the equivalent circuit changes its structure from being primarily an R - L circuit to primarily a back-emf dependent circuit.

Energy Conversion

The energy conversion process in an SRM can be evaluated using the power balance relationship. Multiplying Eq. (13.4) by i on both sides, the instantaneous input power can be expressed as

$$P = V_{ph}i = i^2R + \left(Li \frac{di}{dt} + \frac{1}{2} i^2 \frac{dL}{d\theta} \omega \right) + \frac{1}{2} i^2 \frac{dL}{d\theta} \omega = i^2R + \frac{d}{dt} \left(\frac{1}{2} Li^2 \right) + \frac{1}{2} i^2 \frac{dL}{d\theta} \omega \quad (13.5)$$

The first term represents the stator winding loss, the second term denotes the rate of change of magnetic stored energy, while the third term is the mechanical output power. The rate of change of magnetic stored energy always exceeds the electromechanical energy conversion term. The most effective use of the energy supplied is when the current is maintained constant during the positive $dL/d\theta$ slope. The magnetic stored energy is not necessarily lost, but can be retrieved by the electrical source if an appropriate converter topology is used. In the case of a linear SRM, the energy conversion effectiveness can be at most 50% as shown in the energy division diagram of Fig. 13.3a. The drawback of lower effectiveness is the increase in converter volt-amp rating for a given power conversion of the SRM. The division of input energy increases in favor of energy conversion if the motor operates under magnetic saturation. The energy division under saturation is shown in Fig. 13.3b. This is the primary reason for operating the SRM always under saturation. The term *energy ratio* instead of efficiency is often used for SRM, because of the unique situation of the energy conversion process. The energy ratio is defined as

$$ER = \frac{W}{W + R} \quad (13.6)$$

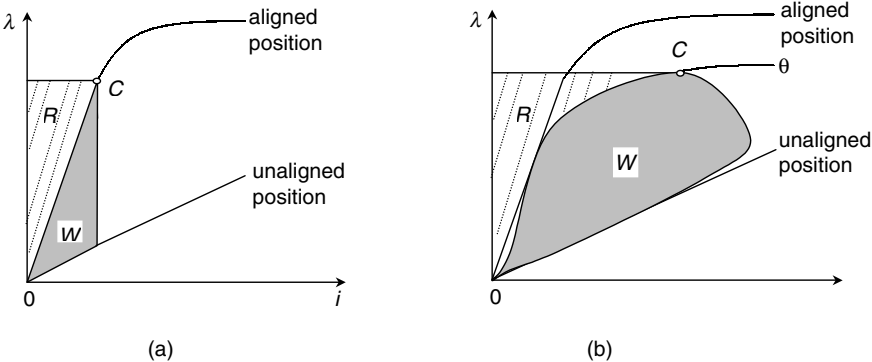


FIGURE 13.3 Energy partitioning during one complete working stroke. (a) Linear case. (b) Typical practical case. W = energy converted into mechanical work. R = energy returned to the DC supply.

where W is the energy converted into mechanical work and R is the energy returned to the source using a regenerative converter. The term energy ratio is analogous to the term power factor used for AC machines.

Torque Production

The torque is produced in the SRM by the tendency of the rotor to attain the minimum reluctance position when a stator phase is excited. The general expression for instantaneous torque for such a device that operates under the reluctance principle is

$$T_{ph}(\theta, i) = \left. \frac{\partial W'(\theta, i)}{\partial \theta} \right|_{i=\text{constant}} \quad (13.7)$$

where W' is the coenergy defined as

$$W' = \int_0^i \lambda(\theta, i) di$$

Obviously, the instantaneous torque is not constant. The total instantaneous torque of the machine is given by the sum of the individual phase torques.

$$T_{inst}(\theta, i) = \sum_{\text{phases}} T_{ph}(\theta, i). \quad (13.8)$$

The SRM electromechanical properties are defined by the static $T-i-\theta$ characteristics of a phase, an example of which is shown in Fig. 13.4. The average torque is a more important parameter from the user's point of view and can be derived mathematically by integrating Eq. (13.8).

$$T_{avg} = \frac{1}{T} \int_0^T T_{inst} dt \quad (13.9)$$

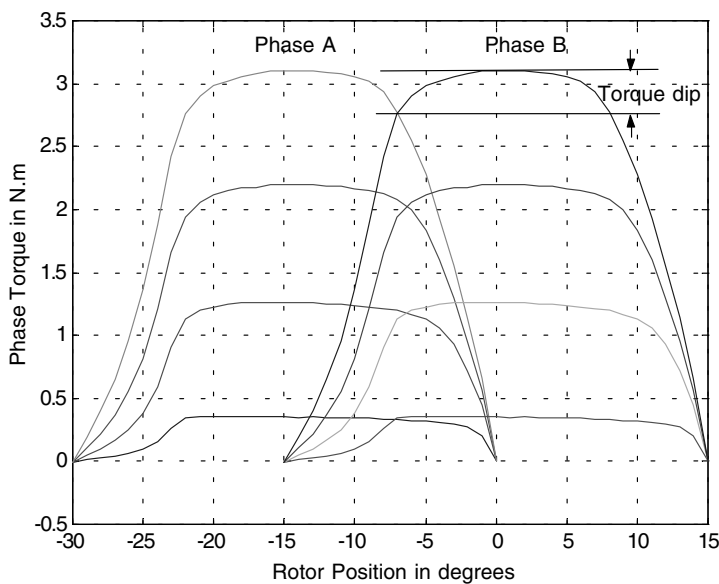


FIGURE 13.4 Torque–angle–current characteristics of a 4-phase SRM for four constant current levels.

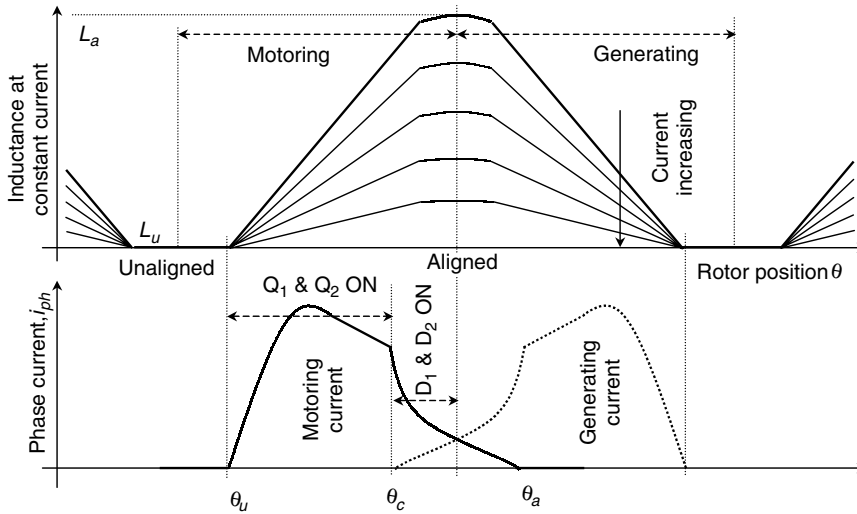


FIGURE 13.5 Phase currents for motoring and generating modes with respect to rotor position and idealized inductance profiles.

The average torque is also an important parameter during the design process.

When magnetic saturation can be neglected, the instantaneous phase torque expression becomes

$$T_{ph}(\theta, i) = \frac{1}{2} i^2 \frac{dL(\theta)}{d\theta} \quad (13.10)$$

The linear torque expression also follows from the energy conversion term (last term) in Eq. (13.5).

The phase current needs to be synchronized with the rotor position for effective torque production. For positive or motoring torque, the phase current is switched such that rotor is moving from the unaligned position toward the aligned position. The linear SRM model is very insightful in understanding these situations. Equation (13.10) clearly shows that for motoring torque, the phase current must coincide with the rising inductance region. On the other hand, the phase current must coincide with the decreasing inductance region for braking or generating torque. The phase currents for motoring and generating modes of operation are shown in Fig. 13.5 with respect to the phase inductance profiles. The torque expression also shows that the direction of current is immaterial in torque production. The optimum performance of the drive system depends on the appropriate positioning of phase currents relative to the rotor angular position. Therefore, a rotor position transducer is essential to provide the position feedback signal to the controller.

Torque–Speed Characteristics

The torque–speed plane of an SRM drive can be divided into three regions as shown in Fig. 13.6. The constant torque region is the region below the base speed ω_b , which is defined as the highest speed when maximum rated current can be applied to the motor at rated voltage with fixed firing angles. In other words, ω_b is the lowest possible speed for the motor to operate at its rated power.

Region 1

In the low-speed region of operation, the current rises almost instantaneously after turn-on, since the back-emf is small. The current can be set at any desired level by means of regulators, such as hysteresis controller or voltage PWM controller.

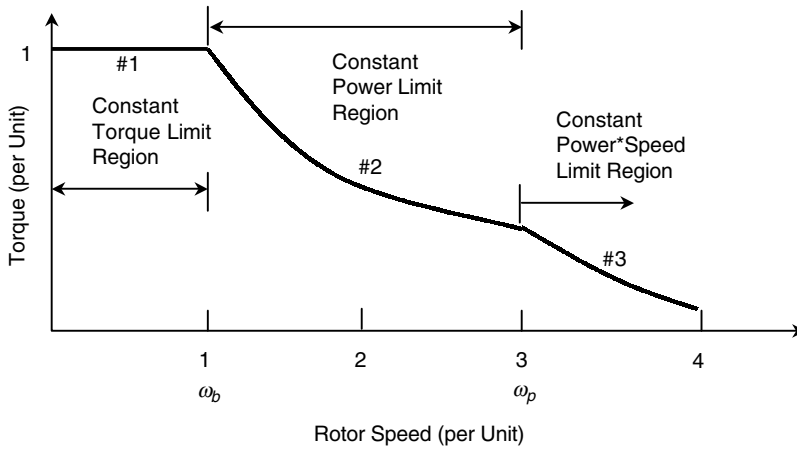


FIGURE 13.6 Torque–speed characteristics of an SRM drive.

As the motor speed increases, the back-emf soon becomes comparable to the DC bus voltage and it is necessary to phase advance the turn-on angle so that the current can rise up to the desired level against a lower back-emf. Maximum current can still be forced into the motor by PWM or chopping control to maintain the maximum torque production. The phase excitation pulses are also needed to be turned off a certain time before the rotor passes alignment to allow the freewheeling current to decay so that no braking torque is produced.

Region 2

When the back-emf exceeds the DC bus voltage in high-speed operation, the current starts to decrease once pole overlap begins and PWM or chopping control is no longer possible. The natural characteristic of the SRM, when operated with fixed supply voltage and fixed conduction angle θ_{dwell} (also known as the dwell angle), is that the phase excitation time falls off inversely with speed and so does the current. Since the torque is roughly proportional to the square of the current, the natural torque–speed characteristic can be defined by $T \propto 1/\omega^2$. Increasing the conduction angle can increase the effective amps delivered to the phase. The torque production is maintained at a level high enough in this region by adjusting the conduction angle θ_{dwell} with the single-pulse mode of operation. The controller maintains the torque inversely proportional to the speed; hence, this region is called the constant power region. The conduction angle is increased by advancing the turn-on angle until the θ_{dwell} reaches its upper limit at speed ω_p .

The medium speed range through which constant power operation can be maintained is quite wide and very high maximum speeds can be achieved.

Region 3

The θ_{dwell} upper limit is reached when it occupies half the rotor pole-pitch, i.e., half the electrical cycle. θ_{dwell} cannot be increased further because otherwise the flux would not return to zero and the current conduction would become continuous. The torque in this region is governed by the natural characteristics, falling off as $1/\omega^2$.

The torque–speed characteristics of the SRM are similar to those of a DC series motor, which is not surprising considering that the back-emf is proportional to current, and the torque is proportional to the square of the current.

13.4 Design

The fundamental design rules governing the choice of phase numbers, pole numbers, and pole arcs were discussed in detail by Lawrenson et al. [2] and also by Miller [3]. From a designer's point of view, the objectives are to minimize the core losses, to have good starting capability, to minimize the unwanted effects due to varying flux distributions and saturation, and to eliminate mutual coupling. The choice of the number of phases and poles is open, but a number of factors need to be evaluated prior to making a selection.

The fundamental switching frequency is given by

$$f = \frac{N}{60} N_r \quad \text{Hz} \quad (13.11)$$

where N is the motor speed in rev/m and N_r is the number of rotor poles. The “step angle” or “stroke” of an SRM is given by

$$\text{Step Angle } \varepsilon = \frac{2\pi}{N_{\text{ph}} \cdot N_{\text{rep}} \cdot N_r} \quad (13.12)$$

The stoke angle is an important design parameter related to the frequency of control per rotor revolution. N_{rep} represents the multiplicity of the basic SRM configuration, which can also be stated as the number of pole pairs per phase. N_{ph} is the number of phases. N_{ph} and N_{rep} together set the number of stator poles.

The regular choice of the number of rotor poles in an SRM is

$$N_r = N_s \pm km \quad (13.13)$$

where k is an integer such that $k \bmod q \neq 0$ and N_s is the number of stator poles. Some combinations of parameters allowed by Eq. (13.13) are not feasible, since sufficient space must exist between the poles for the windings. The most common choice for the selection of stator and rotor pole number for Eq. (13.13) is $km = 2$ with the negative sign.

The torque is produced during the partial overlap region between the stator and rotor pole arcs, and, hence, we must have

$$\min(\beta_r, \beta_s) > \varepsilon$$

where β_r and β_s are the rotor and stator pole arcs, respectively. Practical designs must insure that the rotor interpolar gap is greater than the stator pole arc so that the minimum possible unaligned inductance can be obtained to get the largest possible phase inductance variation between the aligned and unaligned rotor positions. The consideration leads to the second constraint:

$$\frac{2\pi}{N_r} - \beta_r > \beta_s$$

The above constraint prevents simultaneous overlap of one stator pole by two rotor poles.

The angular rate of change of phase flux can be doubled by doubling N_{rep} (while other parameters are held constant with all the coils of each phase connected in series), since this does not affect the maximum and minimum inductances. However, the torque remains unaffected, since the number of turns needs to be halved to keep the back-emf the same when N_{rep} is doubled. Further consideration of the rate of change of flux linkage, available coil area, saliency ratio, split ratio (ratio between rotor radius and motor outside radius), variation in the magnetic circuit reluctance, saturation behavior, and the iron loss due to the increase of the repetition modifies this simplistic conclusion. The advantages of increasing N_{rep}

are greater fault-tolerance and shorter flux-paths leading to lower core losses compared to the single-repetition machines. The contribution to the mean torque can also be increased in multiple repetition machines if the pole width is made more than 50% of that for a single-repetition machine. For $N_{\text{rep}} = 2$, the stator pole width needs to be approximately 70% of that of the single-repetition machine with the optimization criterion of maximizing the co-energy both under high and low current conditions [5]. This gives about 40% more thermally limited torque and horizontal force for the same copper loss and total volume.

The highest possible saliency ratio (the ratio between the maximum and minimum unsaturated inductance levels) is desired to achieve the highest possible torque per ampere, but as the rotor and stator pole arcs are decreased the torque ripple tends to increase. The torque ripple adversely affects the dynamic performance of an SRM drive. For many applications, it is desirable to minimize the torque ripple, which can be partially achieved through appropriate design. The torque dip observed in the $T-i-\theta$ characteristics of an SRM (see Fig. 13.4) is an indirect measure of the torque ripple expected in the drive system. The torque dip is the difference between the peak torque of a phase and the torque at an angle where two overlapping phases produce equal torque at equal levels of current. The smaller the torque dip, the less will be the torque ripple. The $T-i-\theta$ characteristics of the SRM depend on the stator-rotor pole overlap angle, pole geometry, material properties, number of poles and number of phases. A design trade-off needs to be considered to achieve the desired goals. The $T-i-\theta$ characteristics must be studied through finite element analysis during the design stage to evaluate both the peak torque and torque dip values.

Increasing the number of strokes per revolution can alleviate the problem of torque dips and hence the torque ripple. One way of achieving this is with a larger N_r , but the method has an associated penalty in the saliency ratio [2, 3]. The decrease in saliency ratio with increasing N_r will increase the controller volt-amps and decrease the torque output. The higher switching frequency will also increase the core losses. Increasing the phase numbers with a much smaller penalty in the saliency ratio is a better approach for reducing the torque dips. The average torque of the machine will also increase because of the smaller torque dips. The higher number of phases will increase the overlap between phase torques in the regions of commutation. The torque ripple can then be minimized through a controller algorithm that profiles the overlapping phase currents of adjacent phases during commutation. The SRMs with three or lower number of phases suffer more from the problem of torque dips near the commutation region. The four- or five-phase machines can deliver uniform torque without exceedingly boosting the current in rotor positions of low phase-torque per ampere. The cost and complexity of the drive increases with higher phase numbers, since additional switches are required for the power converter. In general, two- or three-phase machines are used in high-speed applications, while four-phase machines are chosen where torque-ripple is a concern.

The inductance overlap ratio K_L , which is the ratio of unsaturated inductance overlap of two adjacent phases to the angle over which the inductance is changing [1, 4], can be utilized during the design phase to analyze the torque characteristics. The ratio gives a direct measure of the torque overlap of adjacent phases. The higher the K_L , the lower will be the torque dip and the higher will be the mean torque as well. Mathematically, the inductance ratio is defined as

$$K_L = 1 - \frac{\varepsilon}{\min(\beta_s, \beta_r)} \quad (13.14)$$

The torque overlap can be increased by widening the stator and rotor poles. Figures 13.7 and 13.8 plot K_L vs. β_s (assuming $\beta_s \leq \beta_r$) and K_L vs. N_{ph} (assuming β_s for $N_{\text{rep}} = 2$ to be 70% of that of β_s for $N_{\text{rep}} = 1$). Figure 13.7 shows that high values of K_L are achievable at relatively low values of β_s for a machine with more phases and/or repetitions. The same machines have better starting capabilities. Also, the rate of change of K_L with respect to β_s is much higher near the minimum possible values for β_s . Additionally, a relatively higher stator pole width will reduce the available window area for winding and increase the copper losses. Therefore, the β_s should not be increased significantly from its minimum possible value. Figure 13.8 shows that the improvement on the problem of torque dip is noticeable in the lower range of N_{ph} .

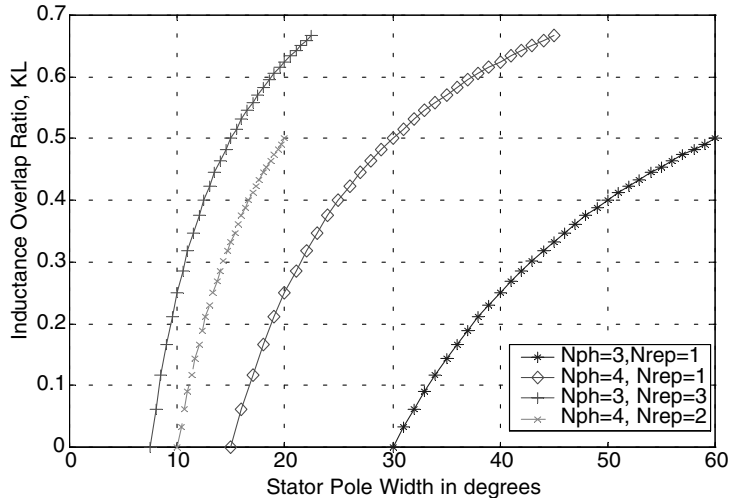


FIGURE 13.7 Inductance overlap ratio vs. stator pole width.

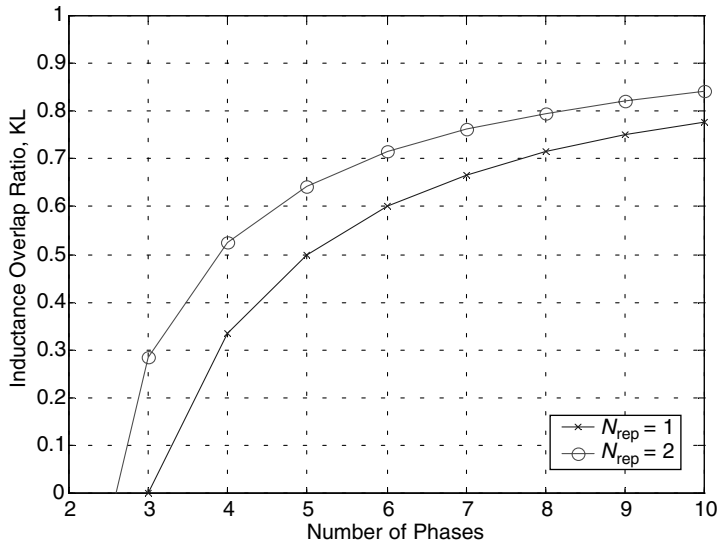


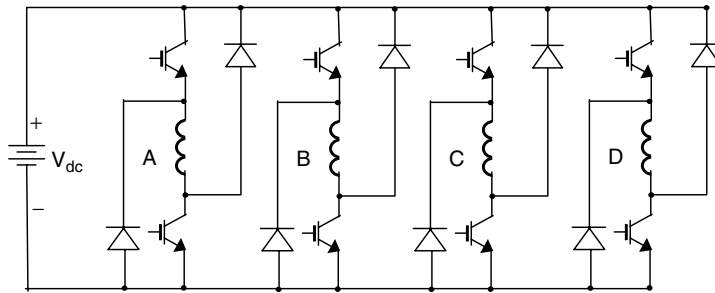
FIGURE 13.8 Inductance overlap ratio vs. number of phases.

13.5 Converter Topologies

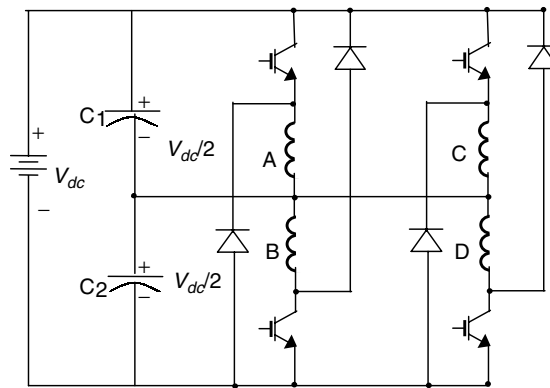
The torque developed in an SRM is independent of the direction of current flow. Therefore, unipolar converters are sufficient to serve as the power converter circuit for the SRM, unlike induction motors or synchronous motors, which require bidirectional currents. This unique feature of the SR motor, together with the fact that the stator phases are electrically isolated from one another, has generated a wide variety of power circuit configurations. The type of converter required for a particular SRM drive is intimately related to motor construction and the number of phases. The choice also depends on the specific application.

The most flexible and the most versatile four-quadrant SRM converter is the bridge converter shown in Fig. 13.9a, which requires two switches and two diodes per phase. The switches and the diodes must

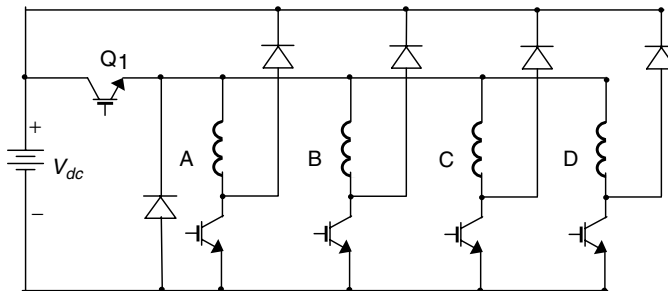
be rated to withstand the supply voltage plus the factor of safety. During the magnetization period, both the switches are turned on and the energy is transferred from the source to the motor. Chopping or PWM, if necessary, can be accomplished by switching either or both the switches during the conduction period according to the control strategy. At commutation both switches are turned off and the motor phase is quickly defluxed through the freewheeling diodes. The main advantage of this converter is the independent control of each phase, which is particularly important when phase overlap is desired. The only



(a)



(b)



(c)

FIGURE 13.9 Converter topologies for SRM: (a) classic bridge power converter; (b) split-capacitor converter; (c) Miller converter.

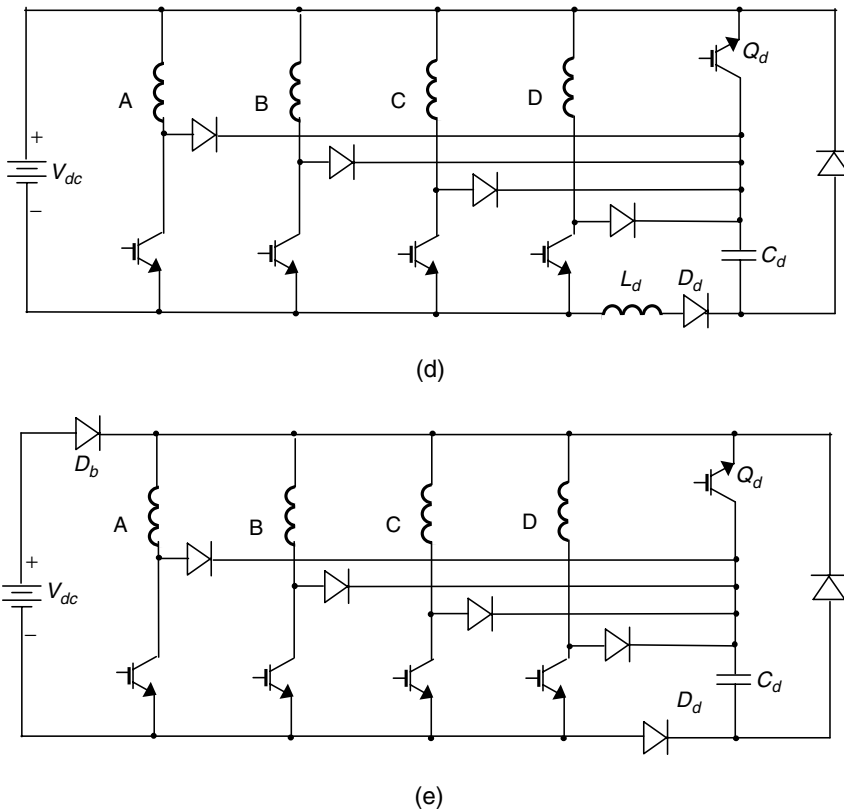


FIGURE 13.9 (Continued) Converter topologies for SRM: (d) energy-efficient converter I; and (e) energy-efficient converter II.

disadvantage is the requirement of two switches per phase. This converter is especially suitable for high-voltage, high-power drives.

The split-capacitor converter shown in Fig. 13.9b has only one switch per phase but requires a split DC supply [6]. The phases are energized through either the upper or the lower DC bus rail and the midpoint of the two capacitors. Therefore, only one half the DC bus voltage can be applied for torque production. To maintain power flow balance between the two supply capacitors, the switching device and the freewheeling diode are transposed for each phase winding, which means that the motor must have an even number of phases. Also, the power devices must be rated to withstand the full DC supply voltage.

The high cost of power semiconductor devices and the need to reduce the switching losses motivated researchers to develop converters with a reduced number of switches. The initial attempt was to solve the problem from the motor side, and the outcome was the bifilar topology, which requires the motor to be wound with a bifilar winding [6]. The complexity in adding the extra winding and the associated increase in motor losses made the topology unpopular.

In low-speed applications, where PWM current control is desirable over the entire range of operation, the bridge converter can be reduced to the circuit shown in Fig. 13.9c developed by Miller. In this converter, chopping is performed by one switch common to all phases. The circuit requires $(n + 1)$ switches for an n -phase motor. The main limitation of this circuit is that at higher speeds the off-going phase cannot be deenergized fast enough because the control switch Q_1 keeps turning on intermittently, disabling forced demagnetization. A class of power converter circuits with fewer than two switches per phase for SR motors having four or more phases has been developed by Pollock and Williams [7].

The energy-efficient C-dump converters I and II are two regenerative converter topologies with a reduced number of switches [8]. The converters are shown in Figs. 13.9d and e. The topologies were derived from the C-dump converter proposed earlier by Ehsani et al. [9]. The energy efficient converter topologies eliminate all the disadvantages of the C-dump converter without sacrificing its attractive features, and also provide some additional advantages. The attractive features of the converters are: lower number of power devices, full regenerative capability, freewheeling in chopping or PWM mode, simple control strategy, and faster demagnetization during commutation. Energy-efficient C-dump converter I has only one-switch forward voltage drop, whereas energy-efficient C-dump converter II has one-switch plus one diode forward voltage drop in the phase magnetization paths. The dump component energy requirements are much lower in these converters compared with those of the C-dump converter.

Converters with a reduced number of switches are typically less fault tolerant compared with the bridge converter. The ability to survive component or motor phase failure should be a prime consideration for high-reliability applications. On the other hand, in low-voltage applications, the voltage drop in two switches can be a significant percentage of the total bus voltage, which may not be affordable. Other factors to be considered in selecting a drive circuit include cost, complexity in control, number of passive components, number of floating drivers required, etc. The drive converter must be chosen to serve the particular needs of an application.

13.6 Control Strategies

Appropriate positioning of the phase excitation pulses relative to the rotor position is the key to obtaining effective performance from an SRM drive system. The turn-on time, the total conduction period, and the magnitude of the phase current determine torque, efficiency, and other performance parameters. The type of control to be employed depends on the operating speed of the SRM.

Control Parameters

The control parameters for an SRM drive are the turn-on angle (θ_{on}), turn-off angle (θ_{off}), and the phase current. The conduction angle is defined as $\theta_{dwell} = \theta_{off} - \theta_{on}$. The complexity of determination of the control parameters depends on the chosen control method for a particular application. The current command can be generated for one or more phases depending on the controller. In voltage-controlled drives, the current is indirectly regulated by controlling the phase voltage.

At low speeds, the current rises almost instantaneously after turn-on because of the negligible back-emf, and the current must be limited by either controlling the average voltage or regulating the current level. The type of control used has a marked effect on the performance of the drive. As the speed increases, the back-emf increases as explained before and opposes the applied bus voltage. Phase advancing is necessary to establish the phase current at the onset of rotor and stator pole overlap region. Voltage PWM or chopping control is used to force maximum current into the motor to maintain the desired torque level. Also, the phase excitation is turned off early enough so that the phase current decays completely to zero before the negative torque-producing region is reached.

At higher-speeds, the SRM enters the single-pulse mode of operation, and control is achieved by advancing the turn-on angle and adjusting the conduction angle. At very high speeds, the back-emf will exceed the applied bus voltage once the current magnitude is high and the rotor position is appropriate, which causes the current to decrease after reaching a peak even though a positive bus voltage is applied during the positive $dL/d\theta$. The control algorithm outputs θ_{dwell} and θ_{on} according to speed. At the end of θ_{dwell} the phase switches are turned off so that negative voltage is applied across the phase to commutate the phase as quickly as possible. The back-emf reverses polarity beyond the aligned position and may cause the current to increase in this region if the current does not decay to insignificant levels. Therefore, the phase commutation must precede the aligned position by several degrees so that the current decays before the negative $dL/d\theta$ region is reached.

In the high-speed range of operation, when the back-emf exceeds the DC bus voltage, the conduction window becomes too limited for current or voltage control and all the chopping or PWM has to be disabled. In this range, θ_{dwell} and θ_{adv} are the only control parameters and control is accomplished based on the assumption that approximately θ_{dwell} regulates torque and θ_{adv} determines efficiency.

Advance Angle Calculation

Ideally, the turn-on angle is advanced such that the reference current level i^* is reached just at the onset of pole overlap. In the unaligned position, phase inductance is almost constant, and, hence, during turn-on back-emf can be neglected. Also, assuming that the resistive drop is small, Eq. (13.4) can be written as

$$V_{ph} = L(\theta) \frac{\Delta i}{\Delta \theta} \omega \tag{13.15}$$

Now, $\Delta i = i^*$ and $\Delta \theta = \theta_{overlap} - \theta_{on} = \theta_{adv}$, where $\theta_{overlap}$ is the position where pole overlap begins, θ_{on} is the turn-on angle and θ_{adv} is the required phase turn-on advance angle. Therefore, we have

$$\theta_{adv} = L_u \omega \frac{i^*}{V_{dc}} \tag{13.16}$$

MacMinn and Sember [10] have described a more sophisticated method of controlling the advance angle, which accounts for the errors due to neglecting the back-emf and the resistive drop in the calculation of θ_{adv} .

Voltage-Controlled Drive

In low-performance drives, where precise torque control is not a critical issue, fixed-frequency PWM voltage control with variable duty cycle provides the simplest means of control of the SRM drive. The early proponents of SRM drives were driven by the fact that a highly efficient variable-speed drive having a wide speed range can be achieved with this motor by optimum use of the simple voltage feeding mode with closed loop position control only. The block diagram of the voltage-controlled drive is shown in Fig. 13.10. The angle controller generates the turn-on and turn-off angles for a phase depending on the rotor speed, which simultaneously determines the conduction period, θ_{dwell} . The duty cycle is adjusted according to the voltage command signal. The electronic commutator generates the gating signals based on the control inputs and the instantaneous rotor position. A speed feedback loop can be added on the outside as shown when precision speed control is desired. The drive usually incorporates a current sensor typically placed on the lower leg of the DC-link for overcurrent protection. A current feedback loop can also be added, which will further modulate the duty cycle and compound the torque–speed characteristics just like the armature voltage control of a DC motor.

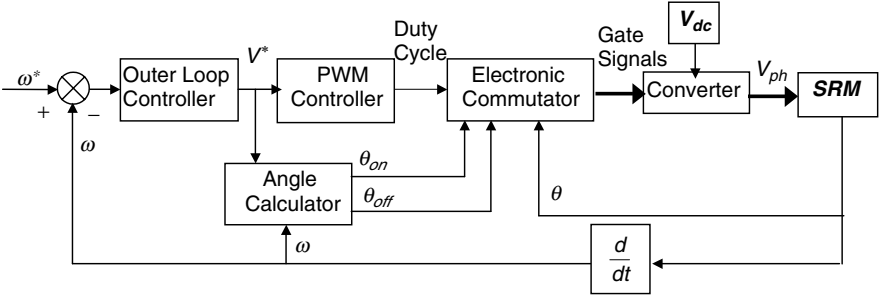


FIGURE 13.10 Voltage-controlled drive.

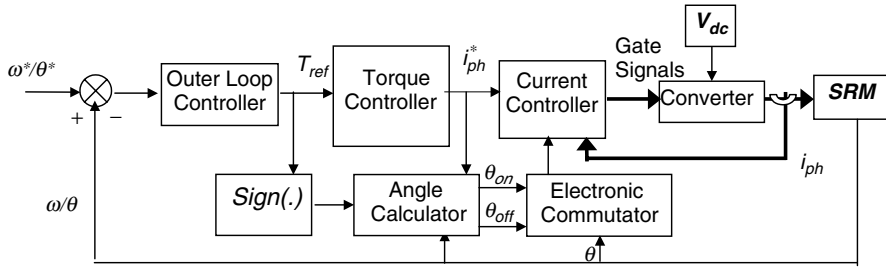


FIGURE 13.11 Current-controlled drive.

Current-Controlled Drive

In torque-controlled drives, such as in high-performance servo applications, the torque command is executed by regulating the current in the inner loop as shown in Fig. 13.11. The reference current i^* for a given operating point is determined from the load characteristics, the speed, and the control strategy. A wide-bandwidth current transducer provides the current feedback information to the controller from each of the motor phases. This mode of control allows rapid resetting of the current level and is used where fast motor response is desired. For loads whose torque increases monotonically with speed such as in fans or blowers, speed feedback can be introduced in the outer loop for accurate speed control.

The simpler control strategy is to generate one current command to be used by all the phases in succession. The electronic commutator (Fig. 13.11) selects the appropriate phase for current regulation based on θ_{on} , θ_{off} , and the instantaneous rotor position. The current controller generates the gating signal for the phases based on the information coming from the electronic commutator. The current in the commutated phase is quickly brought to zero applying negative V_{dc} , while the incoming phase assumes the responsibility of torque production based on the commanded current. The phase transition in these drives is not very smooth, which tends to increase the torque ripple of the drive.

Advanced Control Strategies

A higher performance index, such as torque/ampere maximization, efficiency maximization, or torque ripple minimization can be required in certain applications. For example, in direct drive or traction applications, the efficiency over a wide speed range is critical. For such applications as electric power steering in automobiles, the torque ripple is a critical issue. Typically, the torque/ampere maximization will go hand in hand with efficiency maximization, whereas torque ripple minimization will require the sacrifice of efficiency up to a certain extent.

The high-performance drives will typically be current-controlled drives with sophistication added to the controller as discussed earlier. For efficiency maximization, the key issue is the accurate determination of θ_{on} and θ_{off} , which may require modeling of the SRM and online parameter identification [11]. The modeling issue is equally important for torque ripple minimization, where the overlapping phase currents are carefully controlled during commutation [12, 13]. In these sophisticated drives, the electronic commutator works in conjunction with the torque controller to generate the gating signals. The torque controller will include either a model or tables describing the characteristics of the SRM.

13.7 Sensorless Control

A motor can be a very good sensor of the motion when its voltages and currents possess sufficient information to determine its position and velocity. Compared with other motors, a better position and motion estimator for an SRM is possible because of its double saliency construction. The position estimation is possible even at zero speed, since its inductance/flux varies in accordance with the rotor position. All the published methods of sensorless control of SRM exploit this fundamental idea to extract rotor

position information by measuring either inductance or flux. A wide variety of methods have been proposed to eliminate the rotor position transducer over the past decade, which evolved with their own merits and demerits.

The various methods of indirect-position sensing reported so far in the literature fall under one of the following divisions:

- Phase current monitoring-based estimation [14].
- Phase flux measurement-based position estimation [15].
- Observer-based position estimation (Luenberger observer, sliding-mode observer, Kalman filter, etc.) [16, 17].
- Position estimation by pulse injection into an idle phase [18–21].
- Mutual voltage sensing-based system [22].
- Artificial intelligence-based position estimation (artificial neural network, fuzzy logic, etc.) [23, 24].

The methods of indirect position sensing can be broadly classified into two categories: (1) Nonintrusive methods, where position information is obtained from terminal measurements of voltages and currents and associated computations, and (2) intrusive (or active probing) methods, where low-level, high-frequency signals are injected into an idle phase to determine the position. Further classification of the broad categories is shown in Fig. 13.12.

Nonintrusive methods: The nonintrusive methods rely on the machine characteristics for estimating the rotor position. The terminal measurements of phase voltage or mutual voltage and current are used as inputs for an estimator to obtain the rotor position. The features of the nonintrusive methods are:

- Based on machine characteristics.
- Flux of j^{th} phase is obtained from the integration of flux-inducing voltage,

$$\lambda_j = (v_j - i_j r_j) dt \tag{13.17}$$

- The position information is obtained from flux and phase current information using the machine characteristics:

$$\lambda(i, \theta) \Rightarrow \theta$$

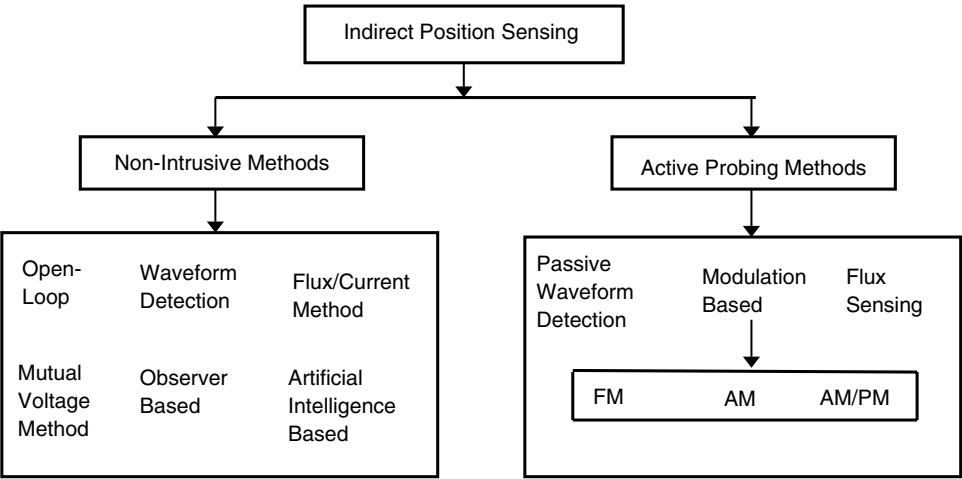


FIGURE 13.12 Classification of indirect rotor-position sensing methods for SRM.

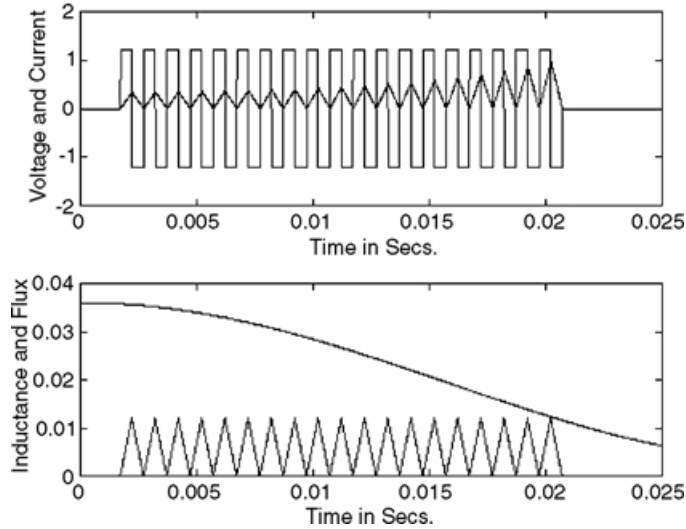


FIGURE 13.13 Rotor position sensing period in a diagnostic phase: (Top trace) applied voltage/20 and phase current; (bottom trace) phase inductance and flux.

- Advantages:
 - Only terminal measurements of phase voltages and currents required.
 - No inherent speed limitation.
 - No diagnostic pulse or extra circuitry needed.
 - Ease of implementation.
- Disadvantages:
 - Mathematical computation may impose some burden on the microprocessor or DSP involved.
 - Performance and accuracy depend highly on the machine model and the performance of the digital integrator.

Intrusive or active probing methods: In active probing methods, an idle or unexcited phase is injected with high-frequency diagnostic signals to obtain the unsaturated phase inductance characteristics, which are related to the rotor position information. The simplicity of these methods is a definite advantage, although inherent speed limitation and generation of negative torque in the sensing phases could be a drawback in some cases. Figure 13.13 shows the sample diagnostic pulses and their variation with rotor position for the active probing method. The appropriate idle phase available at lower to medium speeds is chosen as the diagnostic phase. In the case of a four-phase SRM, the phase diagonally opposite to the active phase has the highest sensitivity of phase current variation with rotor position, and, hence, is chosen as the diagnostic phase. The features of the active probing methods are:

- The position-dependent inductance profile is obtained from measured values of diagnostic pulses as

$$L(\theta) = \frac{V \cdot \Delta t}{\Delta i} \quad (13.18)$$

- The position information is obtained either from a table or simply through comparison with a threshold value.

$$\theta = f^{-1}\{L(\theta)\} \quad (13.19)$$

- Advantages:
 - Well suited for low-speed application.
 - Diagnostic pulse can be injected using the same power converter.
 - Self-starting can be implemented using the same probing pulses.
- Disadvantages:
 - Inherent speed limitations due to the pulse injection.
 - Unnecessary negative torque generation.
 - Needs extra circuitry in some cases, which adds cost and complexity to the overall drive system.

Continuous rotor position information can be obtained from indirect position sensing schemes by a mapping of inductance, flux, or current waveforms to rotor position. Alternatively, the task can be simplified in less sophisticated algorithms by threshold comparison of the indirectly measured position information to effectuate commutation. Phase advancing and retardation is possible by changing the threshold level appropriately.

13.8 Applications

The simple motor structure and inexpensive power electronic requirement have made the SRM an attractive alternative to both AC and DC machines in adjustable-speed drives. An example of SRM application is in heating, ventilation, and air conditioning (HVAC) systems. Here, the high-speed capability, low cost, ruggedness, and fault tolerance features of the SRM drive can produce low-cost adjustable-speed HVAC products for the consumer market. The appliance industry can also benefit from the low-cost and ruggedness of SRM drives. The Maytag Neptune washer uses a three-phase SRM drive for its high-end products. Ametek-Lamb Electric is also commercially manufacturing a heavy-duty vacuum/blower using SRM drives.

SRM drives have great potential for use within the various aspects of conventional automobiles. In this application, the SRM drive can be very simple, inexpensive, compatible with the low battery voltage in the car, very rugged, and fault-tolerant. The absence of temperature sensitivity in the harsh environment under the hood is a definite plus for SRM drives in comparison with permanent magnet motor drives. Example applications of SRMs within an automobile are for the electric power steering and antilock braking systems. The SRM drive is also a strong candidate for the main propulsion drive of an electric or hybrid vehicle. The wide constant power range of SRM drives is especially suitable for such applications. Electric Motorbike, Inc. has developed the Lectra motorcycle based on an SRM drive.

The SRM is also suitable for many industrial and manufacturing applications. For example, high-speed adjustable-speed pumping of fluids for a variety of petrochemical, food processing, and other applications can be done with large horsepower SRM drives. The fact that the SRM can operate under partial converter and motor failure means that these pumps can be placed in critical links in the process control loop. Other high-technology applications for which the SRM drives are being considered include robotic prime movers, aerospace starter/generators, fuel pumps, and servo systems.

Although sophisticated controllers are being designed for SRM drives, it must be realized that the simple PWM voltage control provides a highly efficient variable-speed drive that can be operated over a wide speed range. This mode of operation is usually adequate for a number of motion control applications.

References

1. J. V. Byrne et al., A high performance variable reluctance motor drive: a new brushless servo, in *Motorcon Proc.*, 1985, 147–160.
2. P. J. Lawrenson, J. M. Stephenson, P. T. Blenkinsop, J. Corda, and N. N. Fulton, Variable-speed switched reluctance motors, *IEE Proc. B*, 127(4), 253–265, 1980.

3. T. J. E. Miller, *Switched Reluctance Motors and Their Control*, Magna Physics Publishing, Hillsboro, OH; and Oxford Science Publications, Oxford, U.K., 1993.
4. M. N. Anwar, I. Husain, and A. V. Radun, A comprehensive design methodology for switched reluctance machines, in *IEEE-IAS Annual Conf.*, Rome, Italy, Oct. 2000.
5. H. C. Lovatt and J. M. Stephenson, Influence of the number of poles per phase in switched reluctance motors, *IEE Proc. B*, 139(4), 307–314, 1992.
6. R. M. Davis, W. F. Ray, and R. J. Blake, Inverter drive for switched reluctance motor: circuits and component ratings, in *IEE Proc.*, 128B(2), 126–136, 1981.
7. C. Pollock and B. W. Williams, Power converter circuits for switched reluctance motors with the minimum number of switches, *IEE Proc.*, 137B(6), 373–384, 1990.
8. S. Mir, I. Husain, and M. Elbuluk, Energy-efficient C-dump converters for switched reluctance motors, *IEEE Trans. Power Electronics*, 12(5), 912–921, 1997.
9. M. Ehsani, J. T. Bass, T. J. E. Miller, and R. L. Steigerwald, Development of a unipolar converter for variable reluctance motor drives, *IEEE Trans. Ind. Appl.*, IA-23(3), 545–553, 1987.
10. S. R. MacMinn and J. W. Sember, Control of a switched-reluctance aircraft engine starter-generator over a very wide speed range, in *IECEC Conf. Rec.*, Aug. 1989, 631–638.
11. S. Mir, I. Husain, and M. Elbuluk, Switched reluctance motor modeling with on-line parameter adaptation, *IEEE Trans. Ind. Appl.*, 34(4), 776–783, 1998.
12. K. Russa, I. Husain, and M. Elbuluk, Torque ripple minimization in switched reluctance machines over a wide speed range, *IEEE Trans. Ind. Appl.*, 34(5), 1105–1112, 1998.
13. S. Mir, M. Elbuluk, and I. Husain, Torque ripple minimization in switched reluctance motors using an adaptive fuzzy control, *IEEE Trans. Ind. Appl.*, 35(2), 461–468, 1999.
14. P. P. Acarnley, R. J. Hill, and C. W. Hooper, Detection of rotor position in stepping and switched reluctance motors by monitoring of current waveforms, *IEEE Trans. Ind. Electron.*, IE-32(3), 215–222, 1985.
15. J. P. Lyons, S. R. MacMinn, and M. A. Preston, Flux/Current methods for SRM rotor position estimation, in *IEEE-IAS Annu. Meet.*, Dearborn, MI, 1991, 482–487.
16. A. Lumsdaine and J. H. Lang, State observers for variable-reluctance motors, *IEEE Trans. Ind. Electron.*, IE-37(2), 133–142, 1990.
17. I. Husain, S. Sodhi, and M. Ehsani, Sliding mode observer based control for switched reluctance motors, in *IEEE-IAS Conf. Rec. 94*, Denver, CO, 1994, 635–643.
18. W. D. Harris and J. H. Lang, A simple motion estimator for variable-reluctance motors, *IEEE Trans. Ind. Appl.*, 26(2), 237–243, 1990.
19. S. R. MacMinn, W. J. Rzesos, P. M. Szczesny, and T. M. Jahns, Application of sensor integration techniques to switched reluctance motor drives, *IEEE Trans. Ind. Appl.*, 28(6), 1339–1344, 1992.
20. M. Ehsani, I. Husain, and A. Kulkarni, Elimination of discrete position sensor and current sensor in switched reluctance motor drives, *IEEE Trans. Ind. Appl.*, 28(1), 128–135, 1992.
21. M. Ehsani, I. Husain, S. Mahajan, and K. R. Ramani, New modulation techniques for rotor position sensing in switched reluctance motors, *IEEE Trans. Ind. Appl.*, 30(1), 85–91, 1994.
22. I. Husain and M. Ehsani, Rotor position sensing in switched reluctance motor drives by measuring mutually induced voltages, *IEEE Trans. Ind. Appl.*, 30(3), 665–672, 1994.
23. E. Mese and D. A. Torrey, Sensorless position estimation for variable-reluctance machines using artificial neural network, *IEEE-IAS Annu. Meeting Proc.*, 1, 540–547, 1997.
24. A. D. Cheok and N. Ertugal, Use off fuzzy logic for modeling, estimation, and prediction in switched reluctance motor drives, *IEEE Trans. Ind. Electron.*, 46(6), 1207–1224, 1999.